Inorganic Chemistry

COMMUNICATION

pubs.acs.org/IC

New Oxides Showing an Intense Orange Color Based on Fe^{3+} in Trigonal-Bipyramidal Coordination

Peng Jiang, Jun Li, Arthur W. Sleight, and M. A. Subramanian*

Department of Chemistry, Oregon State University, Corvallis, Oregon 97331, United States

Supporting Information

ABSTRACT: Hexagonal $YIn_{1-x}Fe_xO_3$ phases have been prepared and characterized. The coordination for the In/Fe site in this structure is trigonal-bipyramidal. The colors of the phases change from yellow to orange to dark red with increasing Fe content. Magnetic measurements confirm high-spin Fe^{3+} for all phases.

Many oxides are known with an AMO_3 stoichiometry. The most common structure type for such oxides is the perovskite structure, which is based on close-packed AO_3 layers with all available octahedral sites filled with M cations. The stacking sequence of the AO_3 layers is cubic (ABC), although closely related structures with other stacking sequences are well-known. There is a relatively rare hexagonal AMO_3 structure based on close-packed O layers with a ABACBCA sequence. The A cations occupy all octahedral sites between CA and AC layers, and this site is strongly distorted to a trigonal-antiprismatic coordination. The M cations reside within the BO layers and have a trigonal-bipyramidal coordination. This hexagonal structure in only known for trivalent A cations, which may be In or a small rare earth (Gd to Sc). It is reported that the M cation can be Al, Ga, In, Mn, Fe, 1:1 Cu/Ti, 2:1 Cu/V, or 3:1 Cu/Mo.[1−8] Hexagonal $AMnO_3$ compounds have been of interest as multiferroics because these compounds are ferroelectric and magnetically ordered.[9] The ferroelectric Curie temperatures for these hexagonal AMO_3 compounds are usually about 700 °C. The ferrielectric version of the hexagonal AMO_3 structure is shown in Figure 1. We have recently reported that in the $YInO_3$−$YMnO_3$ solid solution and other closely related systems there are compositions with a brilliant blue color.[10] We also have very recently reported on substitutions in hexagonal $YCu_{0.5}Ti_{0.5}O_3$.[11]

Hexagonal $YFeO_3$ is a metastable compound, which is normally prepared as a powder starting with a solution containing Y and Fe.[12,13] Thin films of hexagonal $YFeO_3$ have also been reported on a ZrO_2−Y substrate.[14] This paper addresses the solid solution between hexagonal $YInO_3$ and $YFeO_3$.

A standard solid-state high-temperature method was used to prepare the In-rich $YIn_{1-x}Fe_xO_3$ phases. The Fe-rich $YIn_{1-x}Fe_xO_3$ phases were prepared by starting with solutions using the citrate method. Experimental details on the synthesis, X-ray diffraction and neutron diffraction, microstructure, and optical and magnetic characterization, and Mössbauer measurements are given in the Supporting Information. LeBail fitting of the X-ray data was carried out using *GSAS* software[15] for the determination of unit cell parameters.

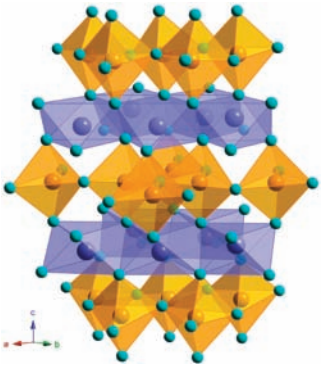

Figure 1. Hexagonal $YIn_{1-x}Fe_xO_3$ powders with ferrielectric structure (Y, blue spheres; In and Fe, orange spheres; O, turquoise spheres).

The standard solid-state synthesis approach was successful for the preparation of hexagonal $YIn_{1-x}Fe_xO_3$ phases from $x = 0.0$ to 0.3. The solution route was successful for the prepartion of $YIn_{1-x}Fe_xO_3$ phases from $x = 0.7$ to 1.0. Neither approach was successful for intermediate x values. The hexagonal unit cell parameters versus x are shown in Figure 2. The scanning electron microscopy (SEM) images in Figure 3 show the much smaller particle size for the Fe-rich samples. Diffuse-reflectance spectra are shown in Figure 4. Plots of magnetic susceptibility are shown in Figure 5, and the results of fitting of these data to the Curie−Weiss law are summarized in Table 1. The experimental moments are in reasonable agreement with the moments expected from high-spin Fe^{3+}.

X-ray diffraction patterns of Fe- and In-rich $YIn_{1-x}Fe_xO_3$ samples are compared in Figure S1 in the Supporting Information. For $x = 0.4$, 0.5, and 0.6 samples, both high- and low-temperature syntheses were tried. For high-temperature synthesis, both perovskite and hexagonal structures are formed. For low-temperature syntheses, In_2O_3 dominates the X-ray pattern.

The broadening of the peaks for the Fe-rich samples is due to the small crystallite size of about 20 nm. All patterns of both the Fe- and In-rich $YIn_{1-x}Fe_xO_3$ samples show the superstructure peaks indicative of the ferrielectric structure shown in Figure 1. Neutron diffraction data for hexagonal $YFeO_3$ had previously been refined for both the ferrielectric and paraelectric structures, but only refined parameters based on the paraelectric form were reported.[13] Both forms gave good fits to the neutron diffraction data, but the X-ray pattern of $YFeO_3$ (see Figure S1 in the Supporting Information) shows a weak reflection indicating the 102 peak that arises from the ferrielectric form. Electron

Received: March 15, 2011
Published: May 31, 2011

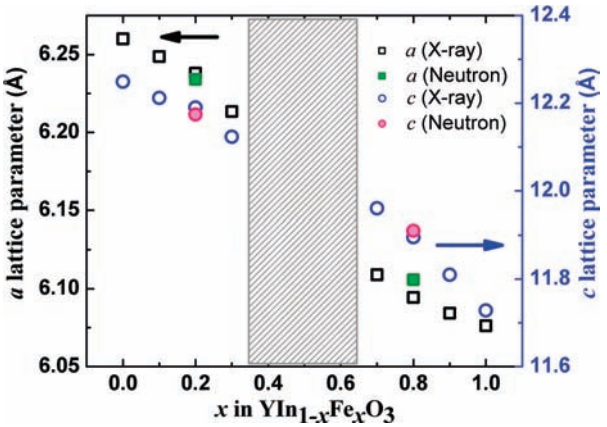

Figure 2. Hexagonal lattice parameters versus x in $YIn_{1-x}Fe_xO_3$. Both X-ray (open symbols) and neutron (solid symbols) data are plotted. The shaded area indicating the discontinuity of the lattice parameters due to missing phases with intermediate x values.

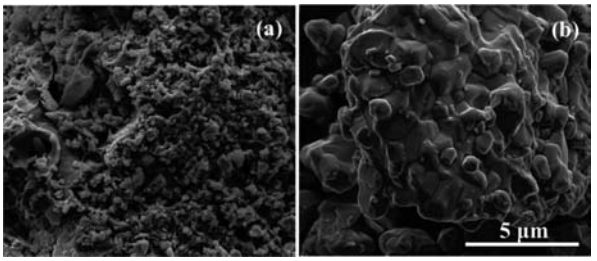

Figure 3. Morphology of $YIn_{1-x}Fe_xO_3$ powders by SEM: (a) $x = 0.9$; (b) $x = 0.1$. The scale is the same for parts a and b.

diffraction studies of hexagonal $RFeO_3$ phases (R = Eu−Lu) have also confirmed this ferrielectric structure.[14] Our low-temperature neutron diffraction patterns of $YFeO_3$ show new peaks (see Figure S2 in the Supporting Information) that can be indexed with the same unit cell used for the room temperature structure, but they violate the space group of the room temperature structure. These new peaks are presumably due to magnetic ordering. Our magnetic susceptibility data for $YFeO_3$ (Figure 5) also suggest magnetic ordering at low temperature.

The colors of oxides containing Fe have been extensively studied, which is, in part, due to the widespread use of various iron oxides as pigments.[16,17] For oxides containing Fe^{3+}, there is strong optical absorption in the near-UV based on a $Fe^{3+}-O^{2-}$ charge-transfer transition. This peak typically extends far enough into the visible to give a yellow color. The lower-energy d−d transitions are forbidden, but they become allowed for various reasons. One of the most important reasons is that in solids the d states broaden into bands. Therefore, a d−d transition is no longer restricted to occurring on one Fe atom. Thus, the d−d transitions become allowed as d states broaden into bands. This broadening increases as the Fe−Fe distances decrease with increasing Fe concentration. In Figure 4, we see the impact on color as the Fe concentration increases. For the $x = 0$ sample ($YInO_3$), there is no absorption in the visible region and the color is white. For $x = 0.1$, the Fe is so dilute that the color is essentially all due to the $Fe^{3+}-O^{2-}$ charge-transfer transition. As the Fe concentration increases, color derived from the lower-energy d−d transitions becomes increasingly more evident (Figure 4).

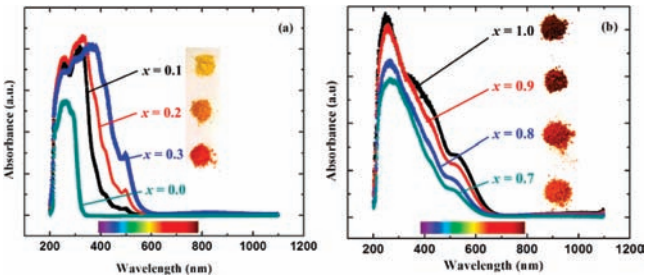

Figure 4. Diffuse-reflectance spectra for $YIn_{1-x}Fe_xO_3$ with colors of the samples varying with x. Spectra for $x = 0$ (hexagonal $YInO_3$: white color) are shown for comparison.

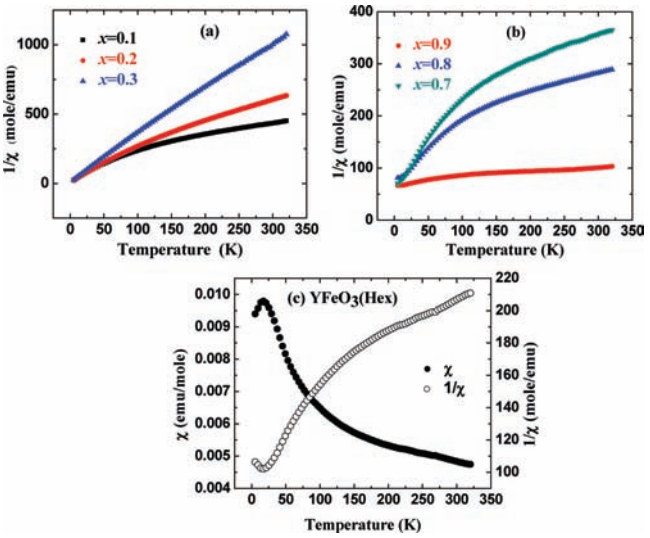

Figure 5. Inverse magnetic susceptibility of $YIn_{1-x}Fe_xO_3$ for (a) $x = 0.1$, 0.2, and 0.3, (b) $x = 0.7$, 0.8, and 0.9, and (c) $x = 1.0$.

Table 1. Magnetic Data for Hexagonal $YIn_{1-x}Fe_xO_3$

x	type	Θ_W	C	μ(calc)	μ(obs)	range (K)[a]
0.1	AFM	−25.68	0.324	1.872	1.610	150−320
0.2	AFM	−96.73	0.655	2.646	2.291	150−320
0.3	AFM	−223.82	1.197	3.243	3.097	150−320
0.7	AFM	−426.77	2.030	4.144	4.032	150−320
0.8	AFM	−489.91	2.787	4.736	4.725	150−320
0.9	AFM	−950.39	3.403	5.616	5.239	250−320
1.0	AFM	−650.23	4.613	5.916	6.078	250−320

[a] The temperature range of the data used for C calculations is shown.

The structure for hexagonal $YFeO_3$ has only one site for Fe. This is true for both the paraelectric and ferrielectric versions of this structure. However, published Mössbauer studies for hexagonal $EuFeO_3$ and $YbFeO_3$ samples (synthesized by the solution method) find two different types of Fe.[18] Room temperature Mössbauer studies on our $YIn_{1-x}Fe_xO_3$ samples also show two Fe sites for Fe-rich samples (synthesized by the solution method) but only one Fe site for In-rich samples made by high-temperature solid-state reactions. The relevant Mössbauer data are shown in the Supporting Information.[19] An obvious difference in the $YIn_{1-x}Fe_xO_3$ system between the In- and Fe-rich samples is

dx.doi.org/10.1021/ic200535c |Inorg. Chem. 2011, 50, 5858–5860

the crystallite size. It would seem that the explanation of the two Fe sites might be related to the small crystallites of the Fe-rich samples. It is well established that phase transitions occurring as a function of the temperature can be influenced by the crystallite size when the size becomes very small. This has been extensively studied both experimentally and theoretically in the case of ZrO_2.[20] The normal room temperature ZrO_2 structure is monoclinic, but this structure transforms to a tetragonal structure at about 1000 °C. The tetragonal form of ZrO_2 is, however, stable at room temperature when crystallites are smaller than 30 nm.[20] A possibility then for our small, Fe-rich $YIn_{1-x}Fe_xO_3$ crystallites is that they are a mixture of the paraelectric and ferrielectric forms. The paraelectric form has a regular trigonal-bipyramidal coordination for Fe. In the ferrielectric form, the three basal plane Fe−O distances are not all equal and the two apical Fe−O distances are not equal. The two different Fe sites in our Fe-rich samples could then arise from the two different phases of the same composition.

Removing the layer of O in the Fe plane (B layer) creates the delafossite structure, where the M cation then has a 2-fold linear coordination. The delafossite structure is known in two modifications, which differ only in the stacking sequence. These are known as the 2H and 3R forms. For some compounds with the delafossite structure such as $ScCuO_2$, both the 2H and 3R forms are known. Intergrowth between the 2H and 3R forms is common and can be regarded as stacking faults.[21] Such stacking faults have been observed in thin films of hexagonal $LuFeO_3$.[14] A very high concentration of stacking faults might also explain the two Fe environments observed by Mössbauer studies.

We are continuing efforts to understand the reason for the occurrence of two Fe sites in hexagonal $RFeO_3$ compounds. These efforts include extensive Mössbauer studies of our Fe-rich $YIn_{1-x}Fe_xO_3$ phases, as well as electron microscopy and Rietveld refinements.

■ ASSOCIATED CONTENT

Ⓢ Supporting Information. Experimental details on the synthesis, powder X-ray diffraction, optical and magnetic data, Mössbauer spectra, and powder neutron diffraction. This material is available free of charge via the Internet at http://pubs.acs.org.

■ AUTHOR INFORMATION

Corresponding Author
*E-mail: mas.subramanian@oregonstate.edu.

■ ACKNOWLEDGMENT

This work was supported by NSF Grant DMR 0804167. We thank Dr. Janet Tate and Dr. Alain Wattiaux for optical measurements and room temperature Mössbauer data. We also thank Dr. Andrew E. Smith for his help with the initial phase of this work. We acknowledge support of the National Institute of Standards and Technology, U.S. Department of Commerce, in providing the neutron research facilities used in this work, and assistance of Dr. Judith Stalick in collecting the neutron diffraction data. The identification of any commercial product or trade name does not imply endorsement or recommendation by the National Institute of Standards and Technology.

■ REFERENCES

(1) Katsufuji, T.; Mori, S.; Masaki, M.; Moritomo, Y.; Yamamoto, N.; Takagi, H. *Phys. Rev. B* **2001**, *64*, 104419.
(2) Yakel, H.; Koehler, W.; Bertaut, E.; Forrat, F. *Acta Crystallogr.* **1963**, *16*, 957.
(3) Van Aken, B. B.; Meetsma, A.; Palstra, T. M. *Acta Crystallogr.* **2001**, *c57*, 230.
(4) Ismailzade, I. G.; Kizhaev, S. A. *Sov. Phys. Solid State* **1965**, *7*, 236.
(5) Pistorius, C. W. F. T.; Kruger, G. J. *J. Inorg. Nucl. Chem.* **1976**, *38*, 1471.
(6) Floros, N.; Rijssenbeek, J. T.; Martinson, A. B.; Poeppelmeier, K. R. *Solid State Sci.* **2002**, *4*, 1495.
(7) Vander Griend, D. A.; Malo, S.; Wang, K. T.; Poeppelmeier, K. R. *J. Am. Chem. Soc.* **2000**, *122*, 7308.
(8) Malo, S.; Maignan, A.; Marinl, S.; Hervieu, M.; Poeppelmeier, K. R.; Raveau, B. *Solid State Sci.* **2005**, *7*, 1492.
(9) Van Aken, B. B.; Palstra, T. T. M.; Filippetti, A.; Spaldin, N. A. *Nat. Mater.* **2004**, *3*, 164.
(10) Smith, A. E.; Mizoguchi, H.; Dlaney, K.; Spaldin, N. A.; Sleight, A. W.; Subramanian, M. A. *J. Am. Chem. Soc.* **2009**, *131*, 17086. Mizoguchi, H.; Sleight, A. W.; Subramanian, M. A. *Inorg. Chem.* **2011**, *50*, 10.
(11) Smith, A. E.; Sleight, A. W.; Subramanian, M. A. *Mater. Res. Bull.* **2011**, *46*, 1.
(12) Yamaguchi, O.; Takemura, H.; Yamashita, M.; Hayashida, A. J. *Electrochem. Soc.* **1991**, *138*, 1492.
(13) Li, J.; Singh, U. G.; Schladt, T. D.; Stalick, J. K.; Scott, S. L.; Seshadri, R. *Chem. Mater.* **2008**, *20*, 6567.
(14) Bossak, A. A.; Graboy, I. E.; Gorbenko, O. Y.; Kaul, A. R.; Kartavtseva, M. S. *Chem. Mater.* **2004**, *16*, 1751.
(15) Larson, A. C.; Von Dreele, R. B. General Structure Analysis System (GSAS). Los Alamos National Laboratory Report LAUR, 2004; pp 86−78. Toby, B. H. *J. Appl. Crystallogr.* **2001**, *34*, 210.
(16) Schwertmann, U.; Cornell, R. M. *Iron Oxides in the Laboratory, Preparation and Characterization*; Wiley-VCH: New York, 2000.
(17) Torrent, J.; Barrón, V. *Encyclopedia of Surface and Colloid Science*;Marcel Dekker: New York, 2002; pp 1438−1446.
(18) Mizoguchi, Y.; Onodera, H.; Yamauchi, H.; Kagawa, M.; Syono, Y.; Hirai, T. *Mater. Sci. Eng.* **1996**, *A217/218*, 164.
(19) Wattiaux, A. Private communication.
(20) Garvie, R. C. *J. Phys. Chem.* **1965**, *69*, 1238.
(21) Li, J.; Yokochi, A.; Sleight, A. W. *Solid State Sci.* **2004**, *6*, 831.